Journal of
Nanoscience and Nanotechnology
Vol. 8, 1–7, 2008

Single Crystalline Molybdenum Nanowires, Nanowire Arrays and Nanopore Arrays in Nickel-Aluminium

Srdjan Milenkovic, Andrew Jonathan Smith, and Achim Walter Hassel*

Max-Planck-Institut für Eisenforschung GmbH, Max-Planck-Str. 1, Düsseldorf, Germany

This work describes a novel fabrication method of single crystalline Mo nanowires and nanowire arrays. The method utilizes directional solidification (*ds*) of a NiAl-Mo eutectic alloy and its subsequent electrochemical processing. In the first step, a self-organized array of Mo nanowires embedded in a NiAl matrix is obtained. By combining the Pourbaix diagrams of the three elements involved, a strategy for selective removal of either of the two phases is derived. An oxidizing acidic solution of pH 0.2 dissolved the matrix and released an array of long and uniform Mo wires. Even a complete extraction of the wires is possible through entire dissolution of the matrix. This method has several advantages. First of all, it is one of the few top-down methods that allow the production of large amounts of nanostructures. In addition, both the wires and the matrix are single crystalline which makes them favorable for various applications. Further, the obtained nanostructures exhibit extremely high aspect ratios (>1000), unreachable by most other techniques. This technique has the potential for the production of nanowire arrays either for employment in sensors or in field emission.

Keywords: Nanowire, Nanopore, Arrays, Eutectic, Molybdenum.

RESEARCH ARTICLE

1. INTRODUCTION

The quest for alternative technologies has stimulated a surge of interest in nanometer-scale materials and devices in recent years. Metal nanowires are one of the most attractive materials because of their unique properties that may lead to a variety of applications. Examples include interconnects for nanoelectronics, magnetic devices, chemical and biological sensors, and biological labels. Metal nanowires are also attractive because they can be readily fabricated with various techniques.

Recently, a novel method of producing metallic nanostructures from directionally solidified and electrochemically treated eutectics has been introduced.[1–3] It surpasses several drawbacks of other available techniques for the fabrication of metallic nanostructures. Firstly, no template or seed is necessary as it is based on self-organization of metallic phases through a diffusion controlled growth. Additionally, both nanowires and nanowire arrays are available. Moreover, very high quantities of nanowires can easily be manufactured.

In this study the novel method was adapted and applied to the NiAl-Mo quasibinary eutectic system. This system has been investigated as a potential candidate for substituting Ni-base superalloys in high temperature applications.[4–16] Microstructure evolution and influence of the growth parameters were the main topics of several publications.[4–6] All studies demonstrated that the directionally solidified NiAl-Mo is of a regular type with fibrous morphology. Further, it was shown that the fiber spacing and diameter are sensitive to chemical composition and processing conditions. However, mechanical properties of the directionally solidified *in-situ* composite such as yield strength, ductility and fracture toughness attracted even more scientific interest.[7–12] As the mechanical compatibility of the constituent phases is an important issue in high temperature applications, only few investigations were devoted to interface characterization including interfacial strength,[13] adhesion,[14] dislocation networks[15] and shear properties.[16] To the best of the authors' knowledge, there is no literature data on using this system in nanotechnology. The NiAl-Mo system has been chosen because it contains Mo as a minor phase, which would yield Mo nanowires. Eutectic alloys that consist of phases with similar structures, such as NiAl-Cr, V, W, often adopt identical growth textures and form a unique orientation relationship between the phases, any lattice parameter mismatch being accommodated by structural dislocations at the interfaces. Walter et al.[17] have extensively studied the NiAl-Cr alloy and various compositional modifications. In the basic alloy

*Author to whom correspondence should be addressed.

the Cr lattice parameter is less than that of NiAl. Additions of Mo, V and W increased and of Fe decreased the Cr lattice parameter. When the lattice parameter of the refractory phase exceeded that of the NiAl, a mixture of faceted rods and lamellae replaced the round fiber morphology of the basic alloy. In each case a unique but different crystallographic orientation relationship was observed.

Molybdenum (Mo) has been an important cathode material for field emission arrays (FEAs), due to its good thermal, mechanical and electrical properties.[18] Mo nanowires have been prepared by electrodeposition of molybdenum oxide nanowires at graphite step-edges as "precursors," and the subsequent reduction of the "precursors" using hydrogen.[19–21] However, the reduction process yields nanowires of low crystallinity and the poor adhesion between nanowires and substrate is limiting their application in devices. For technological applications, it is highly desirable to grow aligned Mo nanowires in a single-step on large-areas and conductive substrates. Recently, Zhou et al. have grown aligned Mo nanowires on stainless steel substrates using high-temperature chemical vapor deposition.[22]

2. EXPERIMENTAL DETAILS

2.1. Eutectic Alloy Preparation

Prealloys were prepared from Nickel (99.97 wt%), electrolytic Aluminum (99.9999 wt%) and Molybdenum (99.99 wt%) by induction melting under an inert Argon atmosphere. They were drop cast into a cylindrical copper mould and subsequently fitted into alumina crucibles. Directional solidification was performed in a Bridgman type crystal growing facility, consisting of the crucible support, cooling ring and heating element (Tungsten net). The alumina crucible with the as-cast ingot was positioned in the furnace and heated up to 1700 °C for initial melting. The heating element was then slowly and uniformly shifted upwards to allow unidirectional heat extraction. This operation was controlled by a servomotor enabling a speed range between 1 and 200 mm h^{-1}. This solidification was conducted at a temperature of 1700 ± 10 °C, a thermal gradient of approximately 40 K cm^{-1} and a growth rate of 30 mm h^{-1}.

2.2. Chemicals and Electrodes

Digestion of the matrix was performed in a mixture of HCl (32%):H_2O_2 (30%):H_2O, 10:10:80. A self made Hg/Hg_2SO_4 reference electrode was used for the polarization experiments. The counter electrode was a strip of Platinum foil with a surface area of 2 cm^2. Polarization was performed in acetate buffer with a pH of 6.0. All chemicals were of p.a. grade and purchased from Merck, Darmstadt, Germany.

2.3. Electronics

Electrochemical investigations of the samples were conducted with a PAR 283 potentiostat/galvanostat manufactured by EG & G. Chemical analysis of the solutions was performed by inductively-coupled plasma optical emission spectrometry (ICP-OES, Thermo). Scanning electron microscopy was performed using a Leo 1550 VP microscope (Leo Elektronenmikroskopie GmbH, Oberkochen, Germany) fitted with an INCA Energy Dispersive System (EDS) (Oxford Instruments, Oxford, UK). In addition, the Automatic Crystal Orientation Mapping-ACOM technique (also known as orientation imaging microscopy, OIM) was used.[23, 24] It is based on the automatic evaluation of electron backscatter diffraction (EBSD) patterns, which are collected by a stepwise scanning of the electron beam on a regular grid over the sample in the SEM. The analysis of the individual EBSD patterns yielded the crystallographic orientations of the crystal at each position of the electron beam. In the present study ACOM has been applied in a high-resolution, high-intensity SEM with a field emission gun (JEOL JSM 6500 F). A high-speed CCD camera (DigiView) for pattern recording and the TSL OIM analysis software was used for ACOM.

3. RESULTS AND DISCUSSION

3.1. Microstructures

Typical microstructure of the directionally solidified NiAl–9Mo alloy grown at 30 mm h^{-1} was fully eutectic devoid of any dendritic regions throughout the cross sections of the specimens, as shown in Figure 1. In the micrographs throughout the paper, the NiAl phase is the matrix and the Mo phase the continuous fibers. The main feature of the eutectic microstructure was the formation of eutectic cells with fine fibrous morphology inside the colony and the coarse regions at the colony boundaries. The formation of the eutectic colony structure has

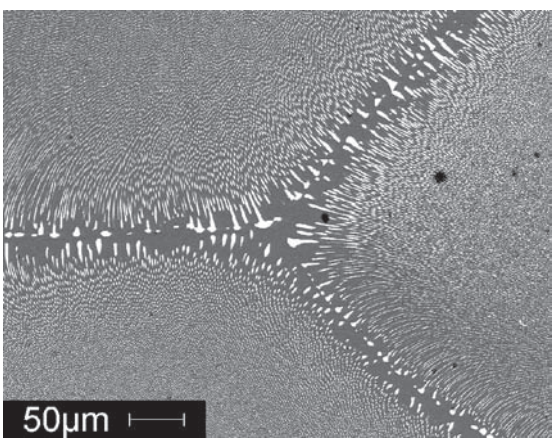

Fig. 1. Cellular eutectic structure of the *ds*–NiAl–Mo alloy grown at 30 mm h^{-1}. The sample was cut in a direction perpendicular to the growth direction and subsequently polished.

RESEARCH ARTICLE

been associated to the combined effects of the impurities rejected from the solidifying eutectic, the growth rate, and the imposed thermal gradient at the solid/liquid interface, which produced a zone of constitutionally undercooled liquid ahead of the growing interface. Under these conditions of growth, the planar solid/liquid interface becomes unstable and transforms into a cellular interface. The growth characteristics of the colony structure have been investigated by several researchers[25–26] and it has been shown that the colonies are formed by the motion of a cellular solid/liquid interface during growth. Further, it was observed that fibers do not grow parallel to each other within the cells, but diverge towards colony boundaries and tend to increase in thickness as they approach it. The direction in which the fibers grow in the cells gives a direct indication of the shape of the growing cellular interface. The formation of a cell structure indicated that the applied growth conditions were below the critical ones for achieving the planar solid/liquid interface. The Mo fibers had a faceted morphology, as shown in Figure 2. The faceted morphology results from the surface energy that is anisotropic for the existing crystallographic orientation relationship between the NiAl and the Mo. Similar morphologies of Gold nanofibres were observed in the Fe–Au eutectoid system.[27, 28] The fiber spacing, defined as the average distance on a transverse section between the centers of adjacent Mo fibers was $\sim 1\ \mu$m and the fiber size, defined as the average edge length of the cross-sections was determined to be 530 nm.

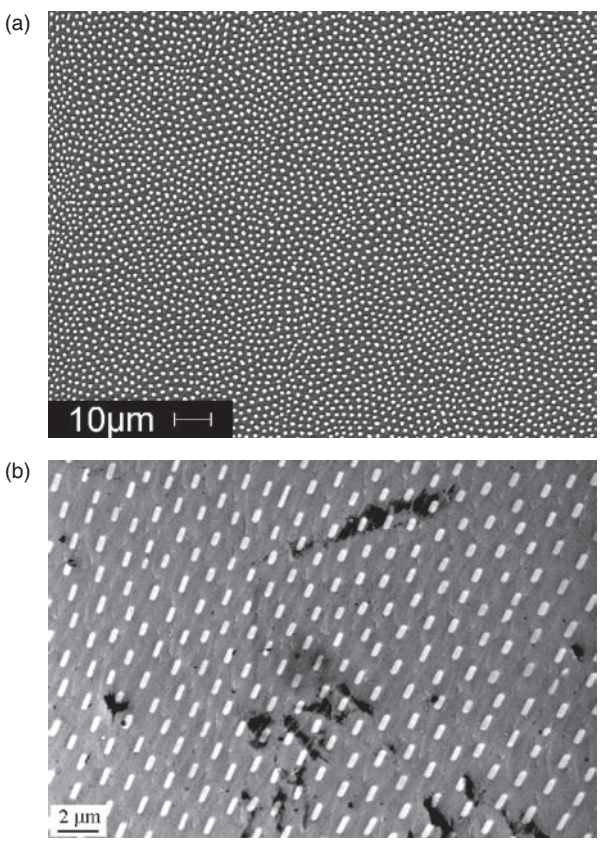

Fig. 2. Morphology of the Mo fibers embedded in the NiAl matrix at different magnifications. See Figure 1 for experimental details.

3.2. Crystallography

An interesting aspect of directionally solidified eutectics is a preferred crystallographic orientation relationship between the phases. The existence of such a specific crystallographic relationship is ascribed to the minimization of the interface energy between the phases. The high degree of thermal stability of many eutectics has also been associated to interfaces of low boundary energies. Cantor[29] has reviewed the evidence for the development of special crystallographic relationships during directional solidification of eutectic alloys and shown that behaviors ranging from strict epitaxial to completely independent growth can occur. Moreover, the propensity for preferred crystallographic relationships and microstructural regularity are not trivially related. The crystallographic relationship between eutectic phases is characterized by the growth direction and the habit plane. The growth direction presents crystallographic axes in each phase parallel to the direction of solidification, while the habit plane is the interface plane between the phases. Considering NiAl based eutectics, only few were characterized regarding crystallographic relationships.[30–34]

In this study orientation imaging microscopy was used to determine the growth direction of the two eutectic phases (NiAl and Mo) and their interfacial planes. EBSD patterns were taken from the individual phases at different locations of the sample. Figure 3 shows the EBSD patterns from the NiAl matrix and the Mo fibers. The growth direction was found to be parallel to ⟨100⟩ directions in both NiAl and Mo. In addition, in both phases planes parallel to interface boundaries were (110) planes. This observation is in agreement with those reported previously.[4, 34]

The (110) habit plane are the closest-packed planes in the *bcc* and B2 crystal structures of Mo and NiAl,[35] respectively. As such, they are frequently selected as interphase boundaries in order to minimize the boundary energies during the eutectic growth. The ratio of the lattice parameters of Mo and NiAl is about 1.09,[35] which suggest that the interface between the NiAl matrix and Mo fibers is semi-coherent.

Comparison of the EBSD patterns of the individual Mo fibers taken at several different positions of the sample showed that the Mo fibers are single crystalline and they have the same crystallographic orientation, even azimuthally. This means that after releasing them from the matrix, a resulting nanowire array would be composed of crystallographically identical Mo single crystals, which might be important for certain applications. Additionally, such an array is very convenient for mechanical, electrical or some other kind of characterization.

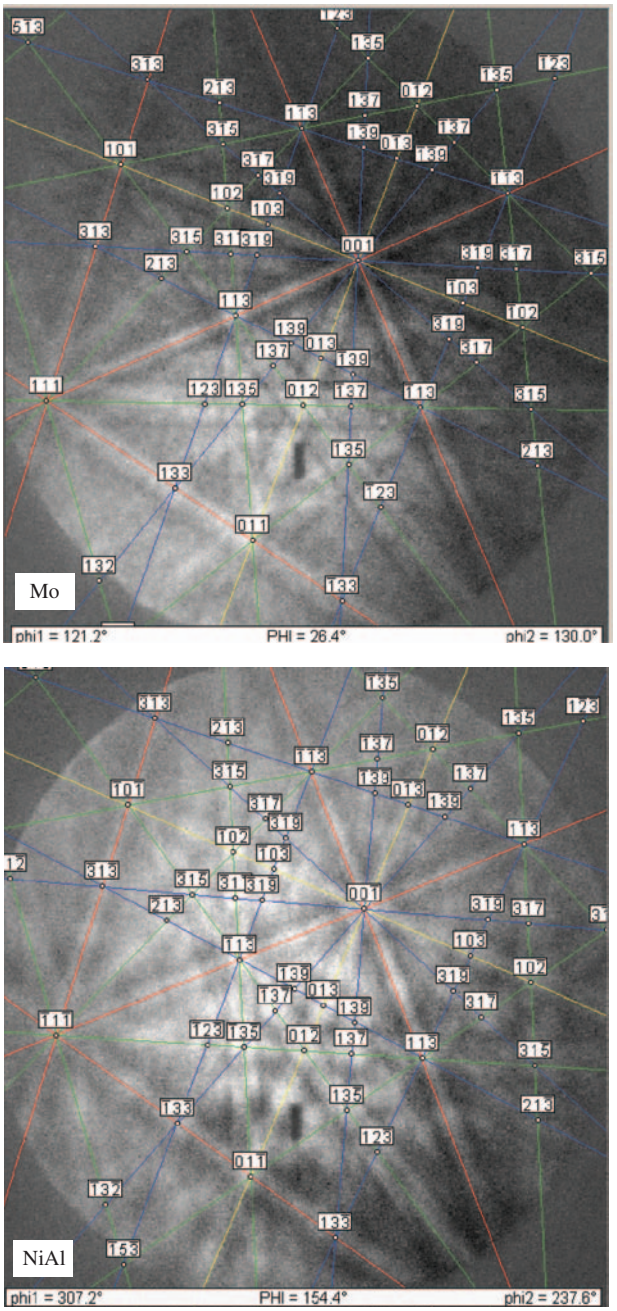

Fig. 3. EBSD patterns from the NiAl matrix and the Mo fibers.

3.3. Electrochemical Processing

In order to derive the optimum conditions for selective dissolution of the matrix as well as the optimum conditions for the selective formation of nanopores or nanochannels through removal of the wires the thermodynamic stability diagrams[36] of the elements in question in aqueous solutions, the so-called Pourbaix diagrams, were combined in Figure 4. The lines in the diagram depict the areas of relative predominance of the different species involved.

In order to extract the Mo wires from the matrix, the conditions under which both matrix elements nickel and

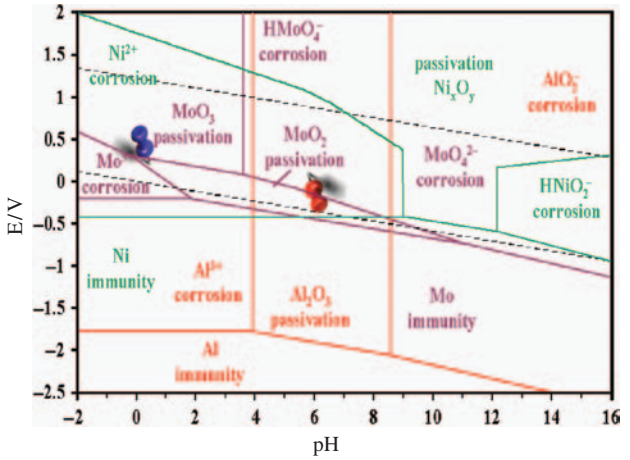

Fig. 4. Combined simplified pH-potential stability diagram derived from Pourbaix diagrams of the three elements Ni, Al and Mo.

aluminum corrode, while the molybdenum passivates were chosen (blue pin at Fig. 4). The samples were immersed in a solution of HCl and H_2O_2 as mentioned previously. A reference electrode was applied to the setup and the potential transient during the selective etching of the NiAl matrix was recorded. This procedure yielded samples with Mo wires protruding from the NiAl matrix (Fig. 5) forming a nanowire array. It can be seen that a large number of nanowires are released from the matrix and are standing upright and parallel. It is important to emphasize that the wire length can be easily controlled by the etching duration.[37] In addition, the selective etching of the matrix provided closer insight into the fiber morphology and enabled examinations of the microstructures in three dimensions. In fact, the large depth of focus of the scanning electron microscope makes it possible to view both the longitudinal and the transverse sections simultaneously, as depicted in Figure 5. This proved the faceted morphology of the molybdenum fibers.

By continuing this process for a few hours the matrix was completely digested so that subsequent filtration yielded free nanowires on a filter paper (Fig. 6). It clearly shows that the wires are very long, reaching the maximum

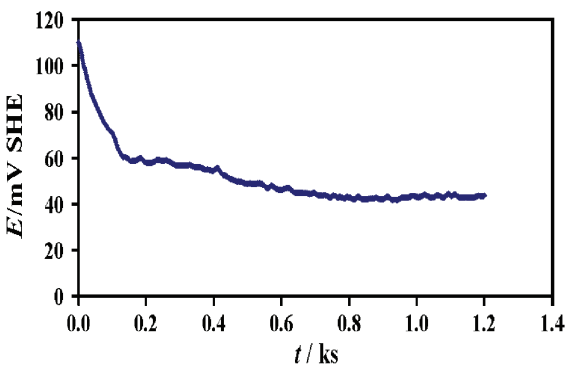

Fig. 5. Potential transient of matrix dissolution of *ds*–NiAl–Mo in a mixture of 3.2% HCl and 3% H_2O_2.

RESEARCH ARTICLE

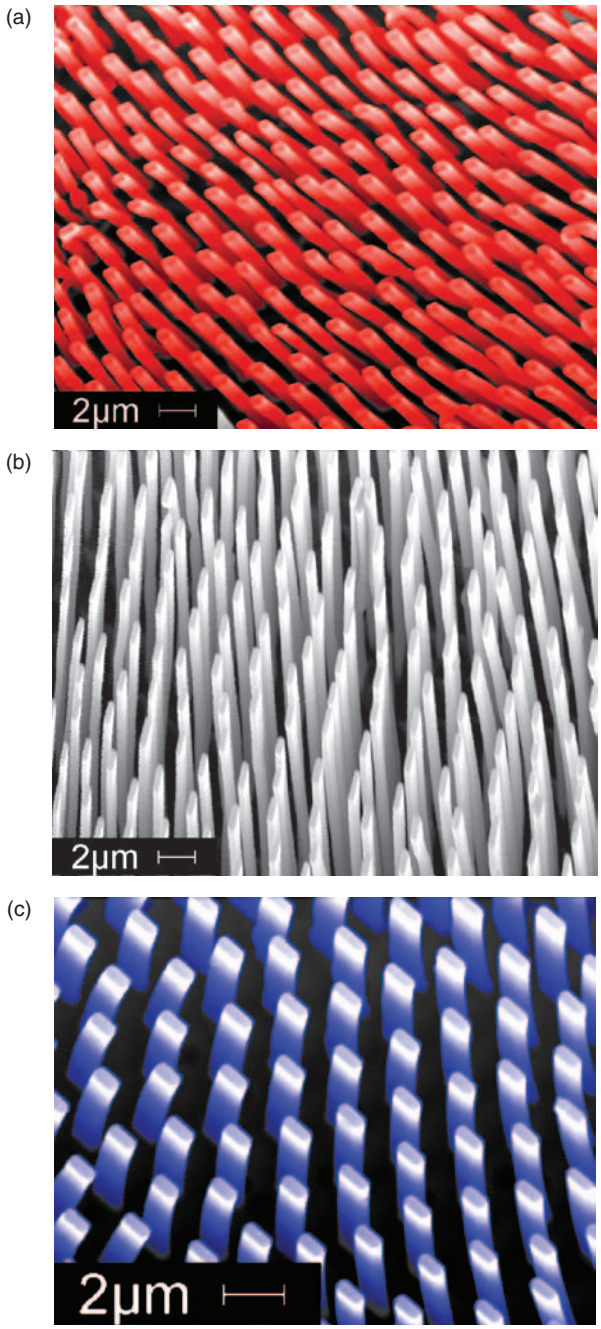

Fig. 6. Array of the Mo nanowires partially released from the NiAl matrix at different magnifications.

length of over 500 μm, and hence, exhibit an extreme aspect ratio of more than 1000. Dissolution of the matrix phase at the free corrosion potential while monitoring this potential with a reference electrode yielded the potential transient shown in Figure 7. After an initial equilibration period the potential stabilizes at a value of about 42 mV SHE. This potential corresponds to the potential of Mo corrosion at a pH of 1.0 just within the "electrochemical window" (Fig. 4).

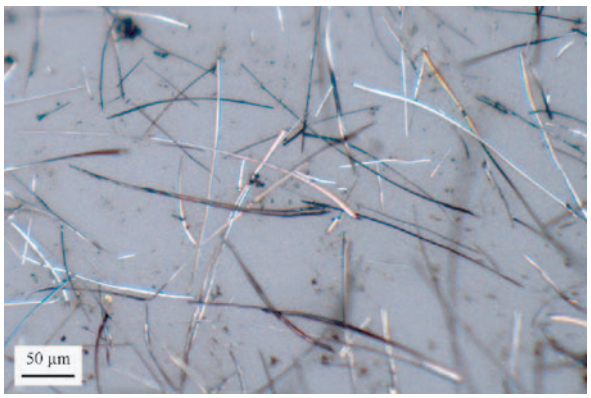

Fig. 7. Mo nanowires on a filter paper after complete dissolution of the matrix.

On the other hand, a selective removal of the Mo phase required completely different conditions which lead to the passivation of the NiAl phase and the corrosion of the Molybdenum (red pin at Fig. 4). In order to passivate Al a mild pH between 4.0 and 8.5 is necessary. Therefore, the samples were immersed in an Acetate buffer with a pH of 6.0 where Al has its solubility minimum. Polarization to a potential of 200 mV SHE yielded an array of pores (Fig. 8). Forming pores by polarizing to 200 mV SHE in the Acetate buffer caused a simultaneous depletion of Ni

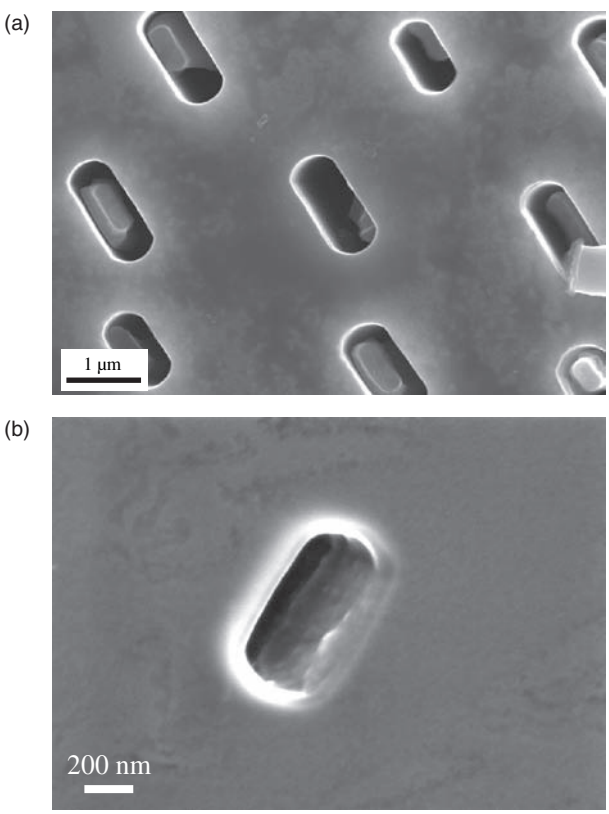

Fig. 8. (a) Nanopore array in a *ds*–NiAl–Mo eutectic alloy after selective electrodissolution of the Mo-minor phase in an acetate buffer (pH 6.0) at 0.2 V (SHE). (b) Close view of a single nanopore.

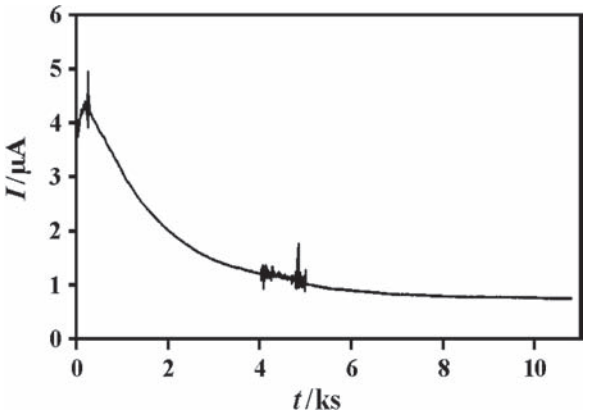

Fig. 9. Current transient of the selective electrodissolution of the Mo nanowires in an acetate buffer (pH 6.0) at 0.2 V (SHE).

in the outermost layer of the samples and the formation of a passive Al_2O_3 layer while the Mo wires were intentionally corroded. Pores are formed in the channels of the embedded molybdenum wires. The pores are evenly distributed across the surface. A closer view into one of these pores is shown in Figure 8(b). The cross section shows that the hole is elongated in one direction; the longer pore diameter is 800 nm and the shorter 400 nm. This structure could be used as a template for electrodeposition of other metals.[38, 39]

Figure 9 shows the current transient of the wire dissolution. The transient shows a steady decrease in current as the pore depth increases. This is probably due to a kinetic hindrance of the dissolution process as a result of the accumulation of dissolved Mo-species in the pores leading to a chemical gradient opposing further dissolution. Due to the high aspect ratio of the pores formed it is difficult to look into these pores. Figure 10 shows a sample that was prepared in the typical procedure used for TEM (transmission electron microscopy). While the perforation in the center part of the figure results from the sample preparation and the local dissolution of both phases a good insight into the successful generation of a nanofilter through the matrix can be seen at the rim. Complete wire dissolution on the entire sample would to allow the production of nanofilters or nanomembranes.

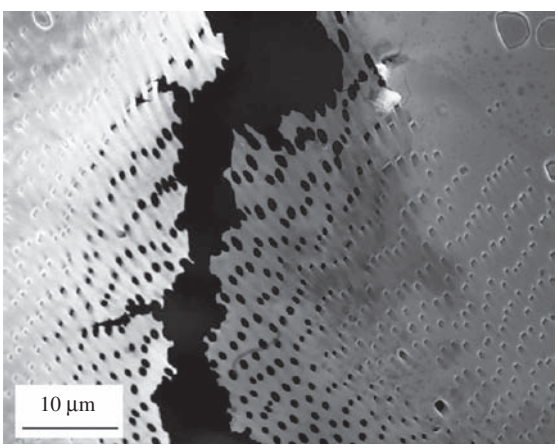

Fig. 10. Nanofilter generation through complete wire dissolution.

4. SUMMARY

Directional solidification of a quasibinary NiAl–Mo eutectic alloy produced Molybdenum fibers embedded in a NiAl matrix. The morphology of the fibers was faceted, with an average cross section of ~530 nm and an interfiber spacing of ~1 μm. Mo nanofibers were proved to be single crystalline having identical crystallographic orientation and cube-on-cube orientation with the matrix.

A strategy for a selective removal of either of the two phases has been derived from a combined Pourbaix diagram of the three elements. Matrix dissolution in a slightly oxidizing acid released an array of long and uniform Mo wires. The high aspect ratio of these wires was demonstrated to be >1000. The wire length could be easily controlled by the etching duration. After complete removal of the matrix and filtration bundles of nanowires were extracted. Producing a large amount of nanowires requires just the corresponding amount of alloy and a modification of the etching time.

Electrodissolution of the Mo with a simultaneous passivation of the NiAl matrix yielded nanopore arrays with rectangular pores Electrodeposition of noble metals such as gold into the pores as it was already demonstrated for the *ds*–NiAl–Re and the *ds*–NiAl–W systems is a promising route for the preparation of sensors.[38, 39] Complete dissolution of Mo fibers would yield a metallic nanofilter or nanomembrane. Such a system would have a number of advantages over ceramic filters as it could be sterilized by electrical resistance heating of the membrane.

Acknowledgments: The financial support of the Deutsche-Forschungs-Gemeinschaft through the project *Production of Nanowire Arrays through Directional Solidification and their Application* within the DFG Priority Programme 1165 Nanowires and Nanotubes—From Controlled Synthesis to Function is gratefully acknowledged.

References and Notes

1. A. W. Hassel, B. B. Rodriguez, S. Milenkovic, and A. Schneider, *Electrochim. Acta* 50, 3033 **(2005)**.
2. A. W. Hassel, A. J. Smith, and S. Milenkovic, *Electrochim. Acta* 52, 1799 **(2006)**.
3. S. Milenkovic, A. W. Hassel, and A. Schneider, *Nano Lett.* 6, 794 **(2006)**.
4. H. Bei and E. P. George, *Acta Mater.* 53, 69 **(2005)**.
5. P. Ferrandini, W. W. Batista, and R. Caram, *J. Alloys and Compounds* 381, 91 **(2004)**.
6. A. Misra, Z. L. Wu, M. T. Kush, and R. Gibala, *Mater. Sci. Eng. A* 239–240, 75 **(1997)**.

7. H. Bei, E. P. George, and G. M. Pharr, *Mater. Sci. Eng., A*, in press **(2007)**.
8. X. H. Du, J. T. Guo, and B. D. Zhou, *Mater. Lett.* 52, 442 **(2002)**.
9. R. S. Sundar, K. Kitazono, E. Sato, and K. Kuribayashi, *Acta Mater.* 49, 1717 **(2001)**.
10. P. Ramasundaram, R. Bowman, and W. Soboyejo, *Mater. Sci. Eng. A* 248, 132 **(1998)**.
11. S. M. Joslin, X. F. Chen, B. F. Oliver, and R. D. Noebe, *Mater. Sci. Eng. A* 196, 9 **(1995)**.
12. X. F. Chen, S. M. Joslin, B. F. Oliver, and C. R. Brooks, *Scripta Metallurgica et Materialia* 29, 1439 **(1993)**.
13. N. I. Medvedeva, Yu. N. Gornostyrev, O. Yu. Kontsevoi, and A. J. Freeman, *Acta Mater.* 52, 675 **(2004)**.
14. J. E. Raynolds, E. R. Roddick, J. R. Smith, and D. J. Srolovitz, *Acta Mater.* 47, 3281 **(1999)**.
15. H. E. Cline, J. L. Walter, E. F. Koch, and L. M. Osika, *Acta Metall.* 19, 405 **(1971)**.
16. S. M. Pickard, H. Zhang, and A. K. Ghosh, *Acta Mater.* 45, 4333 **(1997)**.
17. H. E. Cline and J. L. Walter, *Metallurgical Transactions* 1, 2907 **(1970)**.
18. C. A. Spindt, I. Brodiel, L. Humphrey, and E. R. Westerberg, *J. Appl. Phys.* 47, 5248 **(1976)**.
19. M. P. Zach, K. H. Ng, and R. M. Penner, *Science* 290, 2120 **(2000)**.
20. M. P. Zach, K. Inazu, K. H. Ng, J. C. Hemminger, and R. M. Penner, *Chem. Mater.* 14, 3206 **(2002)**.
21. J. Zhou, N. S. Xu, S. Z. Deng, J. Chen, J. C. She, and Z. L. Wang, *Adv. Mater.* 15, 1835 **(2003)**.
22. J. Zhou, S. Deng, L. Gong, Y. Ding, J. Huang, J. Chen, N. Xu, and Z. L Wang, *J. Phys. Chem. B* 110, 10296 **(2006)**.
23. B. L. Adams, S. I. Wright, and K. Kunze, *Metall. Trans.* 24A, 819 **(1993)**.
24. F. J. Humphreys, *J. Mat. Sci.* 36, 3833 **(2001)**.
25. R. W. Kraft and D. L. Albright, *Trans. Met. Soc. AIME* 221, 95 **(1961)**.
26. H. W. Weart and D. J. Mack, *Trans. Met. Soc. AIME* 212, 664 **(1958)**.
27. S. Milenkovic, A. Schneider, and A. W. Hassel, *Gold Bull* 39, 185 **(2006)**.
28. Y. Chen, S. Milenkovic, and A. W. Hassel, *Nano Lett.*, accepted.
29. B. Cantor, Interphase Interfaces, Grain Boundary Structure and Properties, edited by G. A. Chadwick and D. A. Smith, Academic Press, London **(1976)**.
30. H. E. Cline, J. L. Walter, E. Lifshin, and R. R. Russell, *Met. Trans.* 2, 189 **(1971)**.
31. D. R. Johnson, X. F. Chen, B. F. Oliver, R. D. Noebe, and J. D. Whittenberger, *Intermetallics* 3, 99 **(1995)**.
32. R. Rablbauer, R. Fischer, A Schneider, and G. Frommeyer, *Euromat 2001, Rimini* **(2001)**, p. 48 .
33. Y. X. Chen, C. Y. Cui, J. T. Guo, and D. X. Li, *Mat. Sci. Eng. A* 373, 279 **(2004)**.
34. A. Misra, Z. L. Wu, M. T. Kush, and R. Gibala, *Philos Mag A* 78, 533 **(1998)**.
35. P. Villars and L. D. Calvert, Pearson's Handbook of Crystallographic Data for Intermetallic Phases, American Society for Metals, Metals Park **(1985)**.
36. M. Pourbaix, Atlas of Electrochemical Equilibria in Aqueos Solutions, National Association of Corrosion Engineers, Texas, USA **(1974)**.
37. A. W. Hassel, S. Milenkovic, U. Schürmann, H. Greve, V. Zaporojtchenko, R. Adelung, and F. Faupel, *Langmuir* 23, 2091 **(2007)**.
38. B. B. Rodriguez, A. Schneider, and A. W. Hassel, *J. Electrochem. Soc.* 153, C33 **(2006)**.
39. B. B. Rodriguez and A. W. Hassel, *J. Electrochem. Soc.* in press.

Received: xx Xxxx xxxx. Revised/Accepted: xx Xxxx xxxx.